J. Res. Inst. Catalysis, Hokkaido Univ., Vol. 15, No. 1, pp. 49 to 60 (1967)

CATHODIC SATURATION CURRENT OF THE HYDROGEN EVOLUTION REACTION ON COPPER AND ITS ABSENCE ON MERCURY: PART II. MERCURY

By

Osamu NAGASHIMA*) and Hideaki KITA**)

(Received May 15, 1967)

Abstract

Present work was devoted to the experimental study of absence of cathodic saturation current of hydrogen electrode reaction on mercury as deduced previously from the electrochemical mechanism.

Measurements were conducted on a hanging drop of mercury in sulfuric or hydrochloric acid solution at room temperature. Constant current pulse technique was used to avoid a local heating of electrode and local change of concentration of reactant and product near the electrode at high current density.

Results are as follows. (i) Cathodic build-up curve shows a break at the potential, $V_b = -0.340 \pm 0.020$ V (in r.h.e. scale) in 1N H_2SO_4 and $V_b = -0.52 \pm 0.02$ V in 1N HCl. (ii) TAFEL law was obeyed at high current density up to *ca.* 50 A cm^{-2} reproducing the results of BOCKRIS and AZZAM. (iii) No sign of saturation current was found so far as observed.

The break was attributed to the change of double layer capacity and not to pseudo-capacity due to accumulation of reaction intermediate. Results (i) and (ii) are in harmony with the electrochemical mechanism, while (iii) verifies it.

Introduction

In Part I[1], the hydrogen electrode reaction on copper was studied experimentally and the catalytic mechanism was verified by the existence of the cathodic saturation current. The present part is concerned with the observation of TAFEL plot, namely relation between overvoltage and logarithm of current density, up to the highest possible current density on mercury (*ca.* 50 A cm^{-2}) to test the theoretical inference from the electrochemical mechanism that there exists no cathodic saturation current.

The electrochemical mechanism,

*) Hokkaido Educational University (Iwamizawa), Iwamizawa, Japan.
**) Res. Inst. for Catalysis, Hokkaido University, Sapporo, Japan.

$$2H^+ + e^- \longrightarrow H_2^+(a), \quad H_2^+(a) + e^- \not\longrightarrow H_2, \qquad (1), (2)$$

where (a) signifies the adsorbed state and $\not\longrightarrow$ the rate-determining step respectively, has been supported by HORIUTI and his co-workers[2~4] mainly on the ground of the theoretical inferences in accordance with observations, *i.e.* electrolytic separation factor, 3[3], and the change of TAFEL constant from 1.5 to 0.5 with increase of current density[4]. One of present authors[5] explained on the basis of electrochemical mechanism the relation between logarithm of exchange current density on the metals studied which belong to the groups IIB, IIIB, IVB, and VB in the periodic table and their work function.

HORIUTI *et al.*[6] discussed the TAFEL constant of the electrochemical mechanism as briefly outlined below. The specific rate, $\vec{V}_r/\theta(H_2^+)$, of the rate-determining step (2) is expressed on the basis of the simple model of HELMHOLTZ double layer as[6]

$$\ln\left[\vec{V}_r/\theta(H_2^+)\right] = \alpha F\eta/RT + \text{const.}, \qquad (3)$$

where $\vec{V}_r$ is the uni-directional rate of the rate-determining step, $\theta(H_2^+)$ the covered fraction of electrode surface with $H_2^+(a)$, α a positive proper fraction and η the overvoltage*) respectively. The variation of $\theta(H_2^+)$ with η is derived as follows, provided that the electrostatic potential, E_p, around $H_2^+(a)$ referred to that in the interior of solution, is remaining unchanged with η in accordance with the model of HELMHOLTZ double layer. The preliminary equilibrium of step (1) is stated as

$$\mu^{H_2^+(a)} = 2\mu^{H^+} + \mu^{e^-} \qquad (4.a)$$

in terms of electrochemical potentials of respective species. The electrochemical potential $\mu^{H_2^+(a)}$ is given at sparse population of $H_2^+(a)$ as

$$\mu^{H_2^+(a)} = RT\ln\theta(H_2^+) + \text{const.},$$

and μ^{e^-} as

$$\mu^{e^-} = F\eta + \mu^{e^-}_{rev.}, \qquad (4.b)$$

while μ^{H^+} is constant for a given solution, where $\mu^{e^-}_{rev.}$ is the particular value of μ^{e^-} in the reversible hydrogen electrode. From the above three equations, we have

$$\ln\theta(H_2^+) = F\eta/RT + \text{const.} \qquad (5)$$

Substituting $\ln\theta(H_2^+)$ from Eq. (5) into Eq. (3), we have at low coverage

*) Overvoltage is defined as the negative of potential of test electrode referred to the reversible hydrogen electrode at the same conditions.

$$\ln \vec{V}_r = -\frac{(1+\alpha)F\eta}{RT} + \text{const.}$$

On the other hand, when electrode surface is densely covered with H_2^+(a), $\theta(H_2^+)$ is practically constant independent of η, hence, we have from Eq. (3)

$$\ln \vec{V}_r = \frac{\alpha F\eta}{RT} + \text{const.} \qquad (6)$$

The TAFEL constant,

$$\vec{\tau} = \frac{RT}{F} \cdot \frac{\partial \ln \vec{i}}{\partial \eta},$$

defined in terms of uni-directional current density, $\vec{i}$, proportional to $\vec{V}_r$, is thus $1+\alpha$ or α in the respective case, hence there is no cathodic saturation current as based on the electrochemical mechanism. This inference contrasts with that from the catalytic mechanism, *i.e.* the presence of cathodic saturation current or $\vec{\tau}=0$. The above inference from the electrochemical mechanism was further confirmed later[7] on the basis of an advanced theory of double layer, allowing for ζ-potential of STERN, specific adsorption of H^+(a), H(a) and H_2^+(a) and their non-electrostatic interactions among them.

Experiments are carried out as below to verify the non-vanishing TAFEL constant, even at the highest possible current density on mercury.

Experimental

Experimental methods are the same with those of Part I[1] beside the test electrode.

Mercury was purified, first by bubbling air through it for several days, then by passage through the columns of dilute nitric acid solution and conductivity water, and finally by distillation thrice in vacuum. Spectroscopic analysis (spectrometer, type QF-60, SHIMAZU, Kyoto) of the purified mercury indicated that other metals were less than 10^{-4} wt %. Test electrode was a hanging drop prepared by SHAIN's method[8]. Surface area was calculated from the weight per drop and the density, assuming its spherical shape (*ca.* 0.01 cm^2).

Hydrochloric acid solution occasionally used instead of sulfuric acid solution, was prepared by distilling a concentrated hydrochloric acid upon redistilled water (conductivity, 10^{-6} mho, cm^{-1}) under reduced pressure.

Results and Discussion

Experimental conditions and the values of rest potential are listed in

Table 1. Rest potential is more or less positive as referred to the reversible hydrogen electrode, which may be due to a trace of oxygen in solution and electrode as in the case of copper electrode[1].

TABLE 1. Experimental conditions

No.	Solution	Pre-electrolysis	Temp. (°C)	Rest potential (mV)
1	1N H_2SO_4	6 ma, 90 hrs	22	32.5
2	"	6 ma, 166 hrs	25	70.0
3	"	4 ma, 144 hrs	23	52.5
4	1.4N HCl	6 ma, 114 hrs	25	70.0
5	"	4 ma, 45 hrs	28	< 35.0
6	0.9N H_2SO_4	5 ma, 66 hrs	20	72.5
7	1N H_2SO_4	5 ma, 138 hrs	20	4.0
8	"	5 ma, 42 hrs	20	—
9	"	4 ma, 66 hrs	20	3.5
10	0.9N H_2SO_4	4 ma, 42 hrs	20	< 12.5

Transient

Plate 1 exemplifies cathodic build-up curves obtained with a constant current ($i=6.85\times10^{-2}$ A cm^{-2}) in 1N H_2SO_4 solution. It is noticed from the

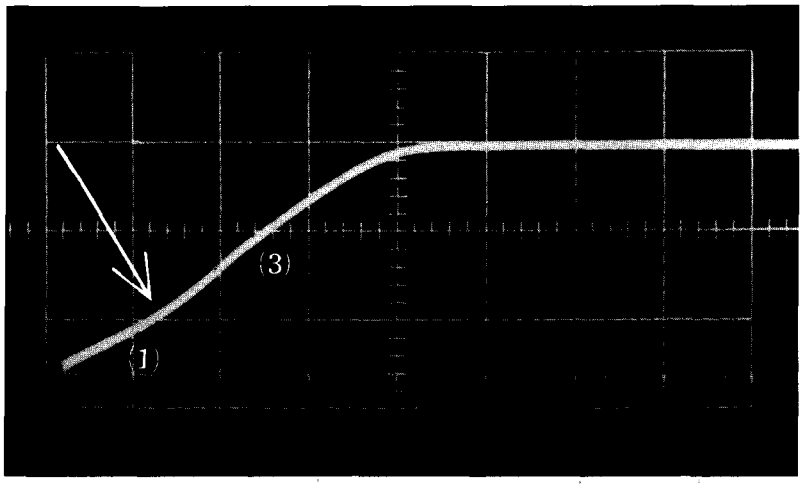

Plate 1. Galvanostatic cathodic build-up curve on mercury in 1N H_2SO_4 solution. i; 6.85×10^{-2} A cm^{-2}, Ordinate; 0.5 V/div, Abscissa; 100 μsec/div. Horizontal trace indicates the potential of the reversible hydrogen electrode at the same conditions.

plate that the curve has a clear break indicated by an arrow, which occurs in all these curves. The potential, V_b, of the break point was found independent of the applied current density at $V_b = -0.340 \pm 0.016$ V (r.h.e. scale) in 1 N H_2SO_4 solution as listed in Table 2. When a build-up curve was started

TABLE 2. Potential of break point (V_b) and capacities (C_{d1}, C_{d2}, C_{d3})

Solution	i (A cm^{-2})	V_b (V)	C_{d1} (μF cm^{-2})	C_{d2} (μF cm^{-2})	C_{d3} (μF cm^{-2})
1 N H_2SO_4 (No. 2 in Table 1)	6.85×10^{-2}	− 0.326	29.5		17.8
	1.47×10^{-1}	− 0.335	34.0		18.6
	2.71×10^{-1}				
	9.0×10^{-1}	− 0.352	28.8		18.7
	1.20	− 0.380	31.6		16.7
	2.66	− 0.320	35.0		19.3
	4.20	− 0.320	33.3		17.2
	6.44	− 0.350	31.0		16.5
	Mean	− 0.340 ± 0.020	31.9 ± 2.1		17.8 ± 0.9
1 N HCl (No. 4 in Table 1)	1.63×10^{-1}			40.7	
	3.26×10^{-1}	− 0.53		36.2	16.5
	6.19×10^{-1}	− 0.50			
	2.14	− 0.52		39.7	17.3
	2.85	− 0.55	32.7	38.9	16.6
	6.19	− 0.55	33.2	37.8	19.3
	1.00×10	− 0.32	34.4	40.0	
	1.53×10	− 0.50		38.7	
	Mean	− 0.52 ± 0.02	33.4 ± 0.7	38.9 ± 1.4	17.4 ± 1.1

from the potential more negative than V_b, no break was observed. Differential capacity was determined from the slope of cathodic build-up curve and the constant current density, by the equation, $C_d = i/(\partial\eta/\partial t)$. Table 2 shows the capacities, C_{d1} and C_{d3}, respectively obtained from parts, (1) and (3), indicated in Plate 1. These capacities are almost constant independent of the applied current density.

The break may be caused by such factor as a change of capacity due to structural change of double layer (*e.g.* reorientation of water molecule), accumulation of reaction intermediate on the electrode surface, or deposition of mercurous ion formed somehow on contact of mercury with solution. The following

considerations lead to the conclusion that the break is due to the first factor, namely, the change of differential capacity of double layer.

The build-up curve has been previously studied by one of present authors[9]. A constant current, i, applied to the test electrode is taken as used; (i) in charging of the double layer, i_d, (ii) in changing the concentration of an adsorbed intermediate formed by discharge steps admitted to be in equilibrium, i_{ads}, and (iii) in the overall electrode reaction, i_f. Thus we have

$$i = i_d + i_{\text{ads}} + i_f ,$$

where

$$i_d = C_d \frac{d\eta}{dt} , \qquad i_{\text{ads}} = C_{\text{ads}} \frac{d\eta}{dt} ,$$

C_{ads} being the pseudo-capacity of adsorption of intermediate. From the above three equations, we obtain[9]

$$\frac{d\eta}{dt} = \frac{i - i_f}{C_d + C_{\text{ads}}} . \tag{7}$$

Eq. (7) gives the basic relationship between η and t in galvanostatic build-up. Let us suppose that the hydrogen electrode reaction proceeds according to the equation

$$i_f = i_0 \left[\exp\left(\frac{F\eta}{2RT} \right) - \exp\left(-\frac{3F\eta}{2RT} \right) \right] , \tag{8}$$

where i_0 is the exchange current density. In the case of the electrochemical mechanism, the above equation is based on the assumption that the step (2) occurs forwards on the densely covered surface with H_2^+ (a), so that TAFEL constant amounts to 0.5 as observed or the forward rate is proportional to the first term in the brackets. It follows from the above assumption that the backward rate is given by the second term in the brackets times i_0*). At full coverage of H_2^+(a), C_{ads} can be neglected in comparison with C_d, since

*) The ratio of forward rate, $\vec{V}$, to the backward rate, $\overleftarrow{V}$, of an elementary reaction is given in terms of the excess of the chemical potential of the initial system, μ^{I}, over that of the final system, μ^{F}, as

$$\vec{V} / \overleftarrow{V} = \exp\left(\frac{\mu^{\text{I}} - \mu^{\text{F}}}{RT} \right) .$$

We have hence particularly for step (2) $\mu^{\text{I}} \equiv \mu^{H_2^+(a)} + \mu^{e^-} = 2\mu^{H^+} + 2\mu^{e^-}$ according to Eq. (4.a), and $\mu^{\text{F}} \equiv \mu^{H_2}$, so that $\mu^{\text{I}} - \mu^{\text{F}} = 2\mu^{H^+} + 2\mu^{e^-} - \mu^{H_2}$ or according to Eq. (4.b), $\mu^{\text{I}} - \mu^{\text{F}} = 2\mu^{H^+} + 2\mu^{e^-}_{\text{rev.}} - \mu^{H_2} + 2F\eta$. Since the sum of first three terms vanishes by equilibrium condition of hydrogen electrode reaction, we have $\mu^{\text{I}} - \mu^{\text{F}} = 2F\eta$, hence $\overleftarrow{V} = \vec{V} \exp(-F\eta/RT)$ or the second term in the brackets of Eq. (8).

$\theta(H_2^+)$ does not depends on η. Thus neglecting C_{ads}, we have from Eqs. (7) and (8) by integration[9],

$$\int_0^{\eta} \frac{d\eta}{i - i_0 \exp(F\eta/2RT) + i_0 \exp(-3F\eta/2RT)} = \frac{t}{C_d}. \qquad (9)$$

The η was calculated as a function of t by Eq. (9) by graphical integration on the base of the numerical values; $i_0 = 2.6 \times 10^{-12}$ A cm^{-2} from the TAFEL line, $C_d = 25.0$ μF cm^{-2} for the range of $\eta < -V_b$ and 17.4 μF cm^{-2} for $\eta > -V_b$, as read from the build-up curve of Plate 1 and $i = 6.86 \times 10^{-2}$ A cm^{-2}. Fig. 1 shows an excellent agreement between the calculated and observed one. The model used here can thus reproduce the observed build-up curve.

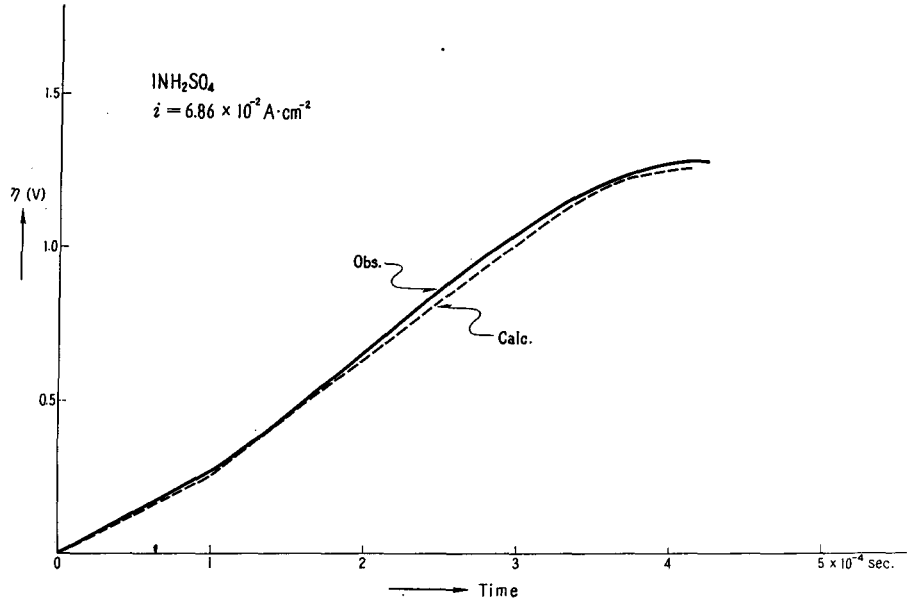

Fig. 1. Comparison of the calculated build-up curve by Eq. (9) with observed one.
——; obs, ----; calc.

The above values of differential capacity at different potential range are qualitatively in harmony with the results of BARKER and FAIRCLOTH[10] who observed by means of triangular polarography $C_d = 35.5$ μF cm^{-2} at $\eta = 0$ and 15.5 μF cm^{-2} at $\eta = 0.7 \sim 0.9$ V in 1N K_2SO_4 solution*) at 25°C as reproduced in Fig. 2. Horizontal lines represent the mean values of differential capacity in Table 2 and length of line indicates potential range at which respective

*) It is known that quite similar results are obtained with solutions of K^+ and H^+ with common anion[11].

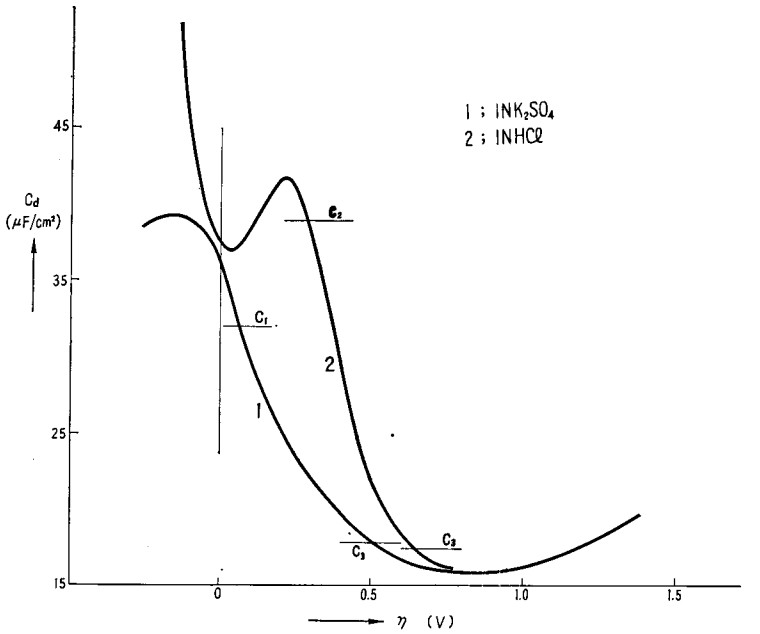

Fig. 2. C_d *vs* η curve reported in 1N K_2SO_4[10] and 1N HCl[15]. Horizontal lines represent mean values of C_{d1}, C_{d2} and C_{d3} in Table 2 and length indicates potential range at which respective values of C_d's are observed.

values are observed. Sharp rise of differential capacity with decrease of η in Fig.2 has been in most cases discussed in terms of structural change of double layer such as reorientation of water molecule and specific adsorption of anion.

The second factor for the break mentioned above, *i.e.* an accumulation of reaction intermediates, cannot be responsible for the break, since it is known that its accumulation with cathodic polarization is associated with very large pseudo-capacity[9,12]; say, more than several hundreds $\mu F\,cm^{-2}$*)at its coverage not close either 1 or 0 and hence it is expected to have much more pronounced break.

The deposition of mercurous ion remaining near the electrode, is excluded from being a factor of the break as follows. If at all, one can expect disappearance of the break in HCl solution because of the extremely small value of its solubility product, *i.e.* $[Hg_2^{\cdot\cdot}][Cl']^2 = 3.5 \times 10^{-18}$ [13] as compared with

*) CONWAY & GILEADI, for example, estimated the pseudo-capacity at 300 or 170 $\mu F\,cm^{-2}$ for the value of 10 or 20 kcal $mole^{-1}$ of a coefficient determing the linear decrease of heat of adsorption with coverage[12]. When the coefficient is zero, the pseudo-capacity amounts to 1600 $\mu F\,cm^{-2}$ at the coverage of 0.5[9].

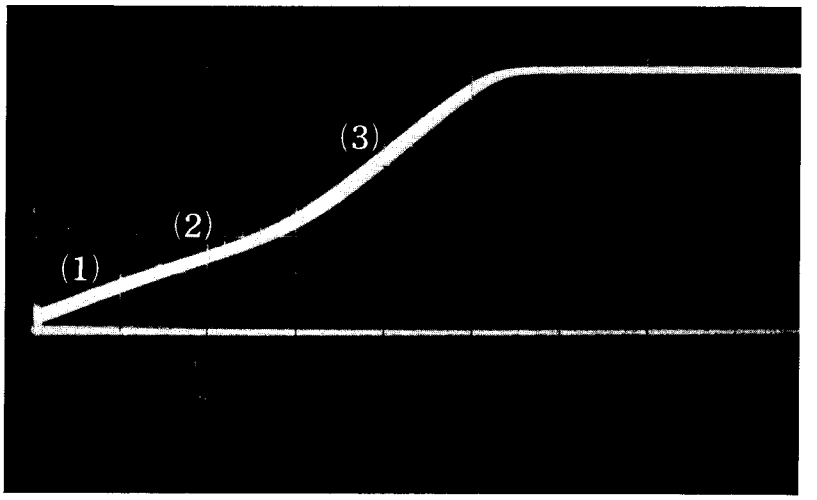

Plate 2. Galvanostatic cathodic build-up curve on mercury in 1N HCl solution. $i=3.26\times10^{-1}$ A cm^{-2}, Ordinate; 0.5 V/div., Abscissa; 10 μsec/div. Horizontal trace indicates the potential of the reversible hydrogen electrode in the same conditions.

$[Hg_2^{\cdot\cdot}][SO_4'']=4.7\times10^{-7}$ [14] in H_2SO_4 solution at 25°C. Plate 2 in 1N HCl solution is substantially similar with Plate 1 in this respect, although somewhat more complicated.

Potential, V_b, at the break point in Plate 2 is practically constant independent of the current density in 1N HCl solution as shown in Table 2. V_b in 1N HCl solution is -0.52 ± 0.02 V on an average, shifting to negative side from that in 1N H_2SO_4 solution. This shift is in the same direction with the shift of the hump in $C_d\sim\eta$ curve as seen from Fig. 2. The build-up curve in 1N HCl solution has a slight tendency of being convex upwards in the region of potential lower than V_b. Table 2 shows differential capacities, C_{d1}, C_{d2} and C_{d3} of parts, (1), (2) and (3), respectively in Plate 2. They are almost constant independent of the applied current density and consistent with $C_d\sim\eta$ curve observed by BOCKRIS *et al.*[15] in 1.0N HCl solution as shown in Fig. 2.

The break observed is thus ascribable to the change of differential capacity of double layer disregarding the effect of accumulation of reaction intermediate or deposition of mercurous ion.

Steady state—TAFEL plot

Observed TAFEL plots are exemplified in Fig. 3 (No. 2 in Table 1). In contrast with the case of copper electrode, no sign of the saturation current

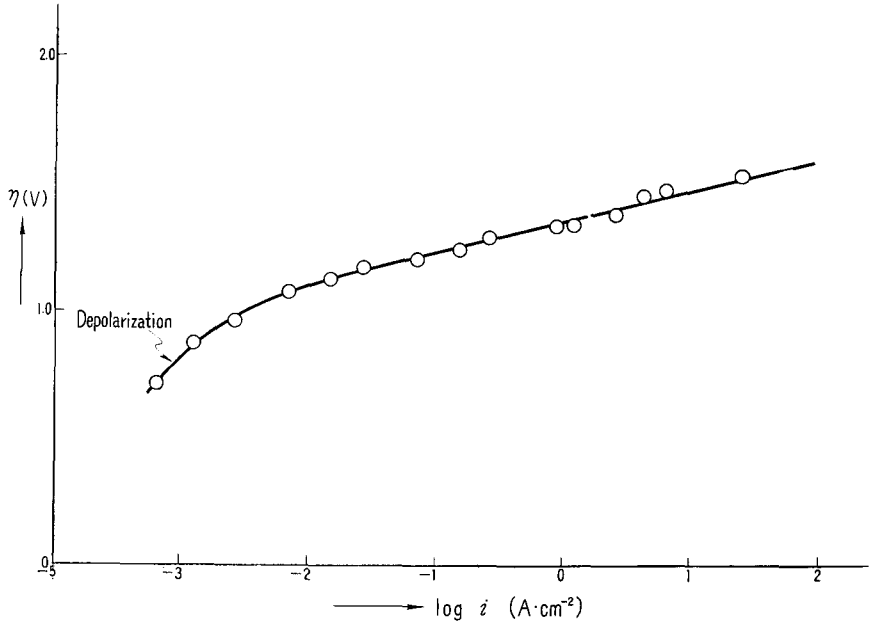

Fig. 3. η *vs* log i curve on mercury in 1N H_2SO_4 at 25°C.
Pre-electrolysis; 6 ma for 170 hrs, Rest potential; +70 mV.

is observed up to the highest possible current density. Linear relation holds down to 10^{-2} or 10^{-3} A cm^{-2}, the further the smaller the rest potential is. TAFEL line is determined by the least square method using 60 points over the current density range of 10^{-2} to 1 A cm^{-2} as

$$\eta\,(\text{Volt.}) = (1.462 \pm 0.017) + (0.124 \pm 0.015) \log i\,(\text{A cm}^{-2}). \qquad (10)$$

Depolarization at low current density as indicated in Fig. 3 may be ascribable to contamination by oxygen, which is inevitable in the present procedure of experiment.

Present results are compared with those of other authors[16~20] in Fig. 4. The observed absence of the cathodic saturation current disproves the catalytic mechanism but verifies the electrochemical mechanism.

The slow discharge mechanism is not disproved by the absence of saturation current. HORIUTI *et al.*[6] have shown, however, that experimental results contradicted the inferences from the slow discharge mechanism; (a) TAFEL constant remaining a proper fraction throughout, (b) too small an activation energy[21] and (c) too large a separation factor[22,23].

The observed value of $\dot{\tau} = 0.5$ of Eq. (6) indicates the saturation of electrode

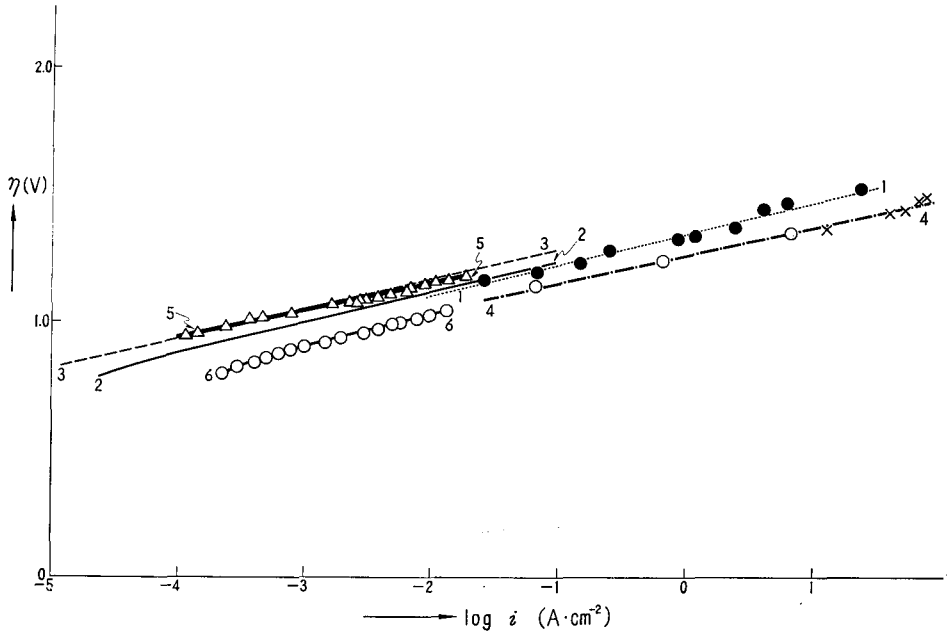

Fig. 4. Comparison of the present results with others.
1; Present result (1N H_2SO_4), 2; DE BETHUNE[16] (1.005N HCl, 25±0.02°C), 3; POST and HISKEY[17] (0.1N HCl, 21±0.1°C), 4; BOCKRIS and AZZAM[18] (5N HCl, 25°C), 5; BUTLER and MAKRIDES[19] (0.1 N $HClO_4$, 25°C), 6; CONWAY cnd SALOMON[20] (1N HCl-CH_3OH, 27°C).

surface with H_2^+(a), which implies that H_2^+(a) is hardly increased by cathodic polarization. This inference is consistent with the conclusion that the break in a cathodic build-up curve is solely ascribable to the change of differential capacity of double layer. It will be of interest to study an anodic build-up curve for further informations on H_2^+(a).

Conclusive Remarks

Hydrogen evolution reaction on mercury electrode was studied at high current density. Absence of the cathodic saturation current was experimentally confirmed, as inferred from the electrochemical mechanism. A break was found in a cathodic build-up curve, which was attributed to the structural change of double layer, rather than to accumulation of reaction intermediate or deposition of mercurous ion.

Acknowledgments

The present authors wish to express their sincere thanks to Emeritus Professor J. HORIUTI, for his discussions given throughout this work.

References

1) O. NOMURA and H. KITA, This Journal, **15**, 45, (1967).
2) J. HORIUTI, T. KEII and K. HIROTA, *ibid*, **2**, 1 (1951-3), J. HORIUTI, *Trans. Symposium Electrode Processes*, edited by E. YEAGER, John Wiley and Sons, Inc., 1961, p. 17.
3) J. HORIUTI and G. OKAMOTO, Sci. Pap. Inst. Chem. Res. Tokyo, **28**, 231 (1936).
4) A. MITUYA, This Journal, **4**, 228 (1956-7).
5) H. KITA, J. Electrochem. Soc., **113**, 1095 (1966).
6) J. HORIUTI, A. MATSUDA, M. ENYO and H. KITA, *Electrochemistry, Proc. First Australian Conference*, held in Sydney, 13-15th February and Hobart, 18-20th February, 1963, Pergamon Press, 1964, p. 750.
7) J. HORIUTI, This Journal, **3**, 52 (1953-5), *Proc. IInd International Congress of Surface Activity*, Vol. II Solid-Gas Interface, Butterworths Sci. Pub., London, 1957, p. 280, A. MATSUDA and J. HORIUTI, This Journal, **6**, 231 (1958).
8) J. D. ROSS, R. D. DEMARS and I. SHAIN, Anal. Chem., **28**, 1768 (1956).
9) J. O'M. BOCKRIS and H. KITA, J. Electrochem. Soc., **108**, 676 (1961).
10) G. C. BARKER and R. L. FAIRCLOTH, Adv. in Polarography, **1**, 313 (1959).
11) K. MÜLLER, private communication.
12) B. E. CONWAY and E. GILEADI, Trans. Faraday Soc., **58**, 2493 (1962).
13) LONDOLT-BÖRNSTEIN, Phy. Chem. Tabellen, 5 Aufrage, HwII, p. 1183.
14) *idem, ibid*, EgIIb, p. 1110.
15) J. O'M. BOCKRIS, K. MÜLLER, H. WROBLOWA and Z. KOVAC, J. Electroana. Chem., **10**, 416 (1965),
16) A. J. BETHUNE, J. Am. Chem. Soc., **71**, 1556 (1949).
17) B. POST and C. F. HISKEY, *ibid.* **72**, 4203 (1950).
18) J. O'M. BOCKRIS and A. M. AZZAM, Trans. Faraday Soc., **48**, 145 (1952).
19) J. N. BUTLER and A. C.MAKRIDES, *ibid.* **60**, 938, (1964).
20) B. E. CONWAY and M. SALOMON, J. Chem. Phys. **41**, 3169 (1964).
21) J. HORIUTI, Z. phys. Chem., N. F. **15**, 162 (1958).
22) T. KEII and T. KODERA, This Journal, **5**, 105 (1957).
23) T. KODERA and T. SAITO, *ibid*, **7**, 5 (1959).